(1963).
[2]R. M. May, Phys. Lett. 25A, 282 (1967).
[3]E. H. Hauge and P. C. Hemmer, Phys. Norv. 5, 209 (1971).
[4]G. Vahala and D. Montgomery, J. Plasma Phys. 6, 425 (1971).
[5]J. B. Taylor, Phys. Lett. 40A, 1 (1972).
[6]G. Joyce and D. Montgomery, J. Plasma Phys. 10, 107 (1973).
[7]C. Deutsch and M. Lavaud, Phys. Rev. Lett. 31, 921 (1973).
[8]S. F. Edwards and J. B. Taylor, Culham Laboratory Report No. P-350 (unpublished).
[9]L. Onsager, Nuovo Cimento, Suppl. 6, 2, 279 (1949).
[10]S. G. Brush, H. L. Sahlin, and E. Teller, J. Chem. Phys., 45, 6, 2102 (1966).
[11]B. R. A. Nijboer and F. W. DeWette, Physica (Utrecht) 23, 309 (1957).
[12]If the interaction potential had been scaled so that $\varphi(x) = -(2e^2/l)\ln(x/l)$, then $\ln V$ in Eq. (7) would have been replaced by $\ln(V/l^2)$. This convention follows from developing the two-dimensional Coulomb interaction as a limit of the three-dimensional interaction of finite-length rods (H. E. DeWitt, private communication).

Measurements of Electron Density Evolution and Beam Self-Focusing in a Laser-Produced Plasma*

L. C. Johnson and T. K. Chu
Plasma Physics Laboratory, Princeton University, Princeton, New Jersey 08540
(Received 2 January 1974)

Space- and time-resolved interferometric measurements of electron density in a CO_2-laser–produced plasma in helium show the development and evolution of radial profiles with on-axis minima, resulting in self-focusing of the laser beam.

The advent of high-power, long-wavelength CO_2 lasers has led to the possibility of achieving controlled thermonuclear fusion by laser heating of magnetically confined plasmas with densities near but below the critical density corresponding to the laser wavelength.[1] One of the fundamental requirements of this reactor scheme is the ability of the plasma to contain the laser beam in a long, thin, linear plasma column. For such containment, plasma refractive properties require that, transverse to the beam axis, the plasma density profile must have an on-axis minimum. We report in the present work measurements of the evolution of the electron-density profile in a laser-produced plasma in the absence of a magnetic field, demonstrating that electron-density profiles favorable for beam containment can be created by the action of the laser beam itself. In addition, beam self-focusing accompanying such favorable density profiles is observed to occur.

The plasma was produced at the focal spot of a TEA (transverse-excitation atmospheric) CO_2 laser with unstable resonator optics in a 5-m confocal cavity, which gives an annular output beam with 5-cm i.d. and 10-cm o.d., pulse energy up to ~30 J, pulse half-power width ~150 nsec, and beam divergence less than 1 mrad. The beam is focused by a KCl lens of 45 cm focal length. The radial intensity distribution at the focal plane is roughly Gaussian, with a measured focal-spot diameter of less than 1 mm, approximately equal to that expected from spherical aberration. The experiments were performed in helium gas at an initial pressure of 30 Torr, which would produce an electron density 2×10^{18} cm^{-3} for complete double ionization, corresponding to $\frac{1}{5}$ the critical density for the 10.6-μm incident CO_2 beam.

Typical plasma luminous images are shown in Fig. 1(a) by the three successive framing pictures, beginning at approximately 10 nsec after gas breakdown with 50 nsec delay between frames. (The incident beam propagates from left to right.) After breakdown the plasma size increases. At a given time, it is approximately cylindrical in shape with a bright shell, and its length along the beam is several times its diameter.

The electron-density measurements were made with a modified Mach-Zehnder interferometer with an internal focus, shown schematically in Fig. 1(b). The beam from a He-Ne laser is focused in the plasma by a lens outside the interferometer, and the recombined beam is monitored with a photomultiplier. One fringe shift corresponds to 3.5×10^{17} electrons/cm^2. When the interferometer is adjusted for uniform intensity across the recombined beam, a linear change of optical path in one arm of the interferometer gives a sinusoidal signal on the photomultiplier. The plasma can be scanned on a shot-to-shot basis by moving either the interferometer lens or

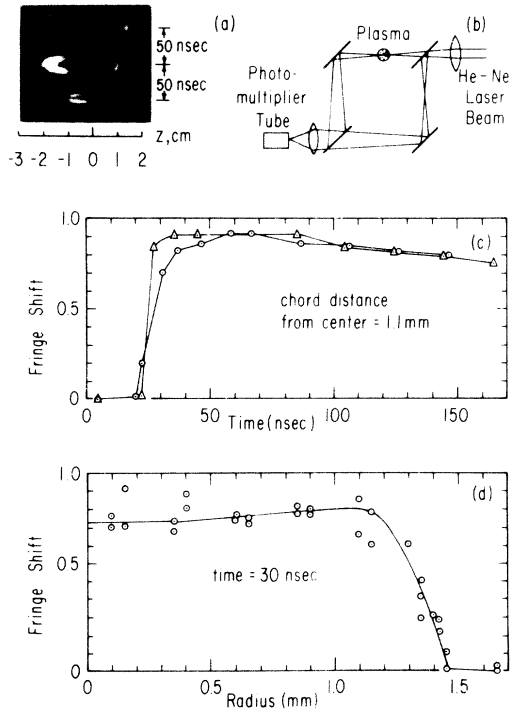

FIG. 1. (a) Framing pictures of the laser-produced He plasma, with first frame approximately 10 nsec after breakdown. CO_2 beam from left to right; focal spot at $z = 0$; initial gas pressure 30 Torr. (b) Diagram of modified Mach-Zehnder interferometer. (c) Time change of fringe shift measured after breakdown, at a chord distance 1.1 mm from center. (d) Fringe-shift profile 30 nsec after breakdown.

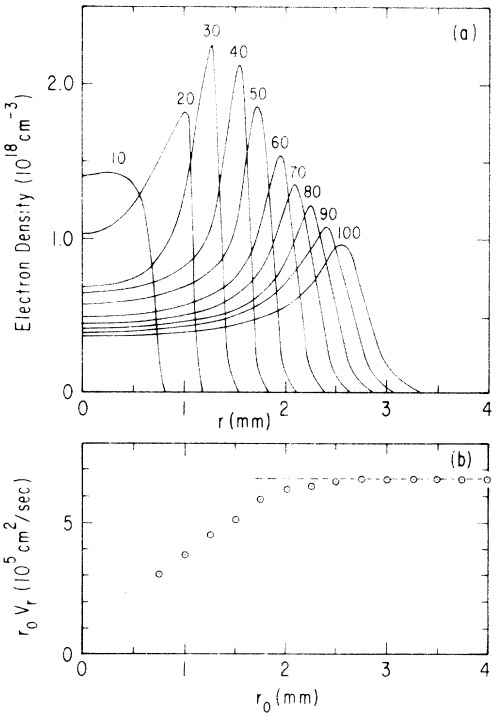

FIG. 2. (a) Electron-density profiles at 10-nsec intervals for the first 100 nsec after breakdown. (b) $r_0 v_r$ versus r_0, where r_0 is the radial shock position and v_r is the radial expansion speed. Dashed line, according to theory for a cylindrical blast wave with an instantaneous energy input.

the CO_2-laser focal spot. The beam waist diameter of the He-Ne laser is about 200 μm, and the time resolution of the measuring system is about 5 nsec. A typical fringe shift, along a chord 1.1 mm out radially from the center of the plasma, is shown in Fig. 1(c), with time measured from the time of breakdown at the focal spot. The two curves are from separate shots and illustrate the reproducibility of measurements. A fringe-shift profile at a given time can thus be constructed from a radial scan of the above measurements. One such profile is shown in Fig. 1(d) at $t = 30$ nsec, with individual points obtained from different shots and the curve representing an average. The radial electron-density profiles can be obtained by Abel inversion.

Radial electron-density profiles in the focal plane of the KCl lens are shown in Fig. 2(a) at 10-nsec intervals for the first 100 nsec after breakdown. At 10 nsec the profile is approximately rectangular with a radius somewhat larger than the measured radius of the focal spot. By 20 nsec, when the plasma diameter is about twice the focal-spot diameter, there is already a deep minimum on axis and a pileup of density at the edge behind a radially expanding shock wave. The measurements are not sufficiently precise to establish clearly the existence or nonexistence of a slight minimum on axis at 10 nsec.

The velocity of the radially expanding shock wave is approximately constant for the first few tens of nanoseconds and varies inversely with the shock radial position (plasma boundary) thereafter. This is illustrated in Fig. 2(b), where the product of the shock position r_0 and the corresponding expansion velocity v_r is plotted versus r_0. The asymptotic behavior ($r_0 v_r = \text{const}$) is characteristic of a cylindrical blast wave. If it is assumed, for purposes of comparison with a similarity solution,[2] that the specific-heat ratio γ of the hot core of the plasma is in the range $\frac{5}{4}$ to $\frac{3}{2}$, then the asymptotic value of $r_0 v_r$, indicated by the dashed line in Fig. 2(b), corresponds to an energy content of 1–2 J/cm. An absolute lower limit on the energy content of the plasma may be obtained by integrating the electron-density pro-

files over the plasma cross section and multiplying by the ionization potential of neutral helium. The result is a monotonic increasing function for the first few hundred nanoseconds, reaching a maximum of 1 J/cm.

Recent numerical solution of one-dimensional magnetohydrodynamic equations for laser-induced heating and radial expansion of a hydrogen plasma[3] reproduce the main features of the measurements shown in Fig. 2(a). The differences between the calculations and measurements, mainly during the first 20 nsec, probably arise from the choice of initial conditions (ionized hydrogen versus neutral helium, details of laser intensity, etc.) and from the fact that the calculations ignore longitudinal variations, as described below. It appears, therefore, that the hydrodynamic model, which assumes laser absorption by classical inverse bremsstrahlung, is essentially correct.

The electron density distribution in the longitudinal direction, inferred from on-axis fringe-shift measurements, is similar to that in the radial direction. After an initial time of ~20 nsec after breakdown at the focal spot, there is pileup of density behind shock waves propagating in both directions along the beam axis. The axial-shock propagation speed is higher than that in the radial direction, consistent with the axial and lateral plasma size shown in the framing pictures of Fig. 1(a). This is because, in the longitudinal direction, plasma behind the shock absorbs beam energy and further propels the shock. The relative speeds of the two laser-supported detonation waves propagating longitudinally from the focal spot depend upon the initial gas pressure. In general, with higher filling pressure a larger fraction of the beam intensity will be absorbed by the wave propagating up the beam toward the laser and less energy will be available to drive the wave propagating away from the laser. We note that in laser-induced gas breakdown at high pressure,[4] such that the plasma frequency is near or above the laser frequency, there exists only one laser-supported detonation wave, propagating toward the focusing lens.

Refractive effects for 10.6-μm radiation should be pronounced in the large density gradients near the boundary of the expanding plasma. These effects may result in beam containment in the density trough. To observe these beam self-focusing effects directly, we made use of the fact that the unstable resonator produces an annular laser beam. Two detectors were arranged to sample the beam transmitted through the focal region, as shown in Fig. 3(a). Detector A, situated in the hollow region of the annular cone, should receive no illumination from the transmitted laser beam in the absence of refraction, while detector B samples the undeflected beam. The upper photograph of Fig. 3(b) shows signals from the two detectors with the gas chamber evacuated. As expected, the on-axis detector A receives no signal, and detector B records the incident pulse shape. With plasma, when detector B shows sudden attenuation of the transmitted beam due to gas breakdown, detector A shows a signal which persists until the end of the laser pulse.

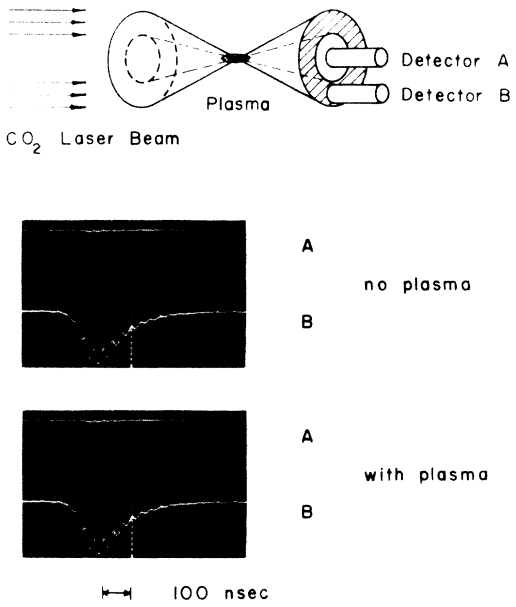

FIG. 3. Measurement of a self-focused beam. (a) Beam geometry near the focal spot and arrangement of beam detectors. The unstable resonator optics of the CO_2 laser gives an annular beam which, when focused, gives an annular cone. (b) Detector signals for cases with and without plasma.

By imaging the plasma region outside the gas chamber, it was established that, beginning approximately 50 nsec after breakdown, the refracted signal emanates from the end of the cylindrical plasma, indicating that the plasma column functions as a light pipe for radiation entering at the opposite end. In the top two image-converter pictures of Fig. 1(a), the point from which the trapped beam emerges from the plasma appears as a bright spot on the right side.

Several important considerations arise from the present experiment. First, the action of the

laser itself can produce plasma-density profiles favorable for beam focusing. Thus, a laser-heated reactor may not require establishing favorable density profiles beforehand, e.g., with a θ pinch.[5] Second, it may be anticipated that in the presence of a longitudinal magnetic field to inhibit radial expansion, higher self-focused beam intensity and increased plasma heating will result. Third, the laser-supported detonation wave propagating toward the focusing lens continuously produces a high-density, low-temperature front which absorbs beam energy and thus reduces the energy of the beam transmitted through the front. This beam-shielding effect, which substantially reduces the beam intensity in the plasma interior, and which is expected to occur in plasmas with preionization as well, must be minimized if efficient laser heating of a long, thin plasma column is to be achieved.

It is a pleasure to thank Mr. J. Fitzwilliam for his able assistance in performing Abel inversion, and Mr. W. Johns for technical assistance.

*Work supported by the U.S. Atomic Energy Commission Contract No. AT(11-1)-3073.

[1]J. M. Dawson, R. E. Kidder, and A. Hertzberg, Princeton University Plasma Physics Laboratory, MATT Report No. 782, 1971 (unpublished); J. M. Dawson, A. Hertzberg, R. Kidder, G. Vlases, H. Ahlstron, and L. Steinhauer, in *Proceedings of Fourth European Conference on Plasma Physics and Controlled Nuclear Fusion* (Comitato Nazionale per l'Energia Nucleare, Ufficio Edizioni Scientifiche, Roma, Italy, 1970).

[2]L. I. Sedov, *Similarity and Dimensional Methods in Mechanics* (Academic, New York, 1959), pp. 210–251.

[3]N. H. Burnett and A. A. Offenberger, to be published.

[4]S. A. Ramsden and W. E. R. Davies, Phys. Rev. Lett. 13, 227 (1964); Yu. P. Raizer, Zh. Eksp. Teor. Fiz. 48, 1508 (1965) [Sov. Phys. JETP 21, 1009 (1965)].

[5]R. Turner and T. Poehler, Phys. Fluids 13, 1072 (1970); N. A. Amherd and G. C. Vlases, Bull. Amer. Phys. Soc. 18, 1326 (1973).

Dynamical Spin Susceptibility of the Anderson-Morel State in Superfluid He^3

Kazumi Maki
Department of Physics, Tohoku University, Sendai, Japan

and

Hiromichi Ebisawa
Department of Applied Science, Tohoku University, Sendai, Japan

(Received 4 May 1973)

Making use of a model Hamiltonian which includes, in addition to the pairing interaction, the spin-exchange interaction as well as the dipole interaction, we calculate explicitly the dynamical spin susceptibility of the Anderson-Morel state. It is shown within the random-phase approximation that the spin susceptibility has simple poles, which give rise to the nuclear magnetic resonance in liquid ^{3}He. The result is compared with a recent phenomenological theory by Leggett.

Recent experiments[1-4] have established that liquid ^{3}He undergoes a second-order phase transition around 2.7 mK. Furthermore the observation of a shift in the NMR frequency by Osheroff *et al.*[2] in the A phase has stimulated much theoretical investigation.[5-7] Making use of a sum-rule argument, Leggett[5] calculated the shift of the squares of the resonance frequency, which appears to account at least qualitatively for the observed shift.

We study here theoretically the dynamical spin susceptibility of the Anderson-Morel (AM) state[8] in the superfluid state. For this purpose we start with the following Hamiltonian:

$$H = H_0 + H_Z + H_I + H_d , \tag{1}$$

where H_0 includes the kinetic energy and the BCS-like pairing energy, H_Z is the Zeeman energy in the presence of a magnetic field H (along the z axis), H_I is the spin-exchange energy as introduced currently in the paramagnon model,[9] and finally H_d is the dipole interaction energy.[5]

Although in the previous discussion[5] of the NMR shift in superfluid ^{3}He, the spin-exchange energy is not mentioned explicitly, it is of pri-

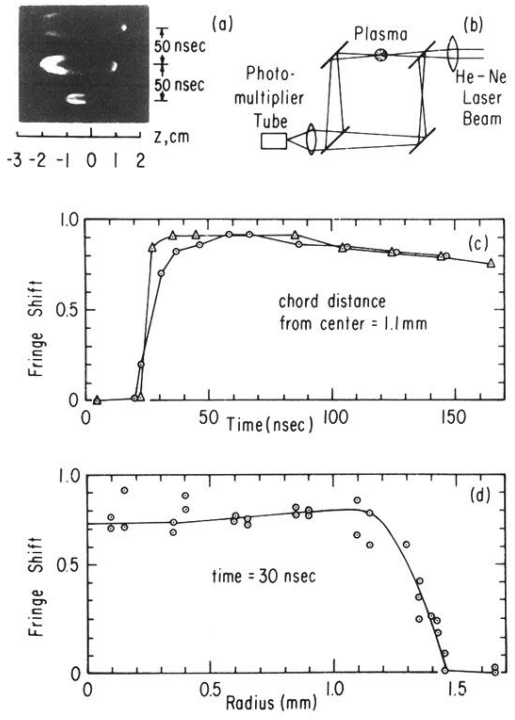

FIG. 1. (a) Framing pictures of the laser-produced He plasma, with first frame approximately 10 nsec after breakdown. CO_2 beam from left to right; focal spot at $z = 0$; initial gas pressure 30 Torr. (b) Diagram of modified Mach-Zehnder interferometer. (c) Time change of fringe shift measured after breakdown, at a chord distance 1.1 mm from center. (d) Fringe-shift profile 30 nsec after breakdown.

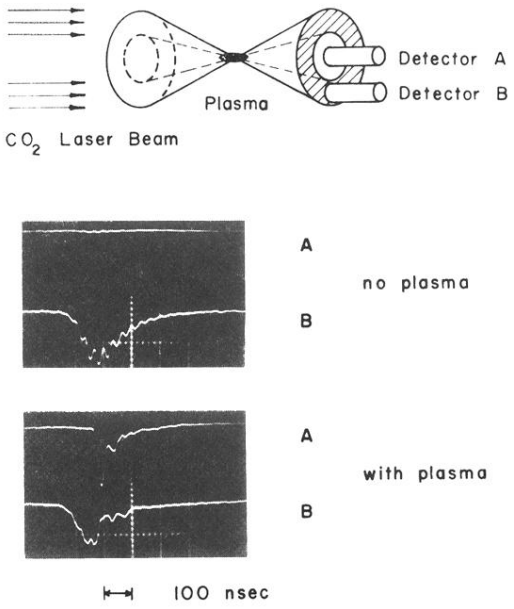

FIG. 3. Measurement of a self-focused beam. (a) Beam geometry near the focal spot and arrangement of beam detectors. The unstable resonator optics of the CO_2 laser gives an annular beam which, when focused, gives an annular cone. (b) Detector signals for cases with and without plasma.